Ping Pong Beam Training for Multi Stream MIMO Communications with Hybrid Antenna Arrays

Nabil Akdim[1], Carles Navarro Manchón[2], Mustapha Benjillali[3], and Elisabeth de Carvalho[2]

[1] Intel Deutschland, Munich, Germany
[2] Department of Electronic Systems, Aalborg University, Denmark
[3] Communication Systems Department, INPT, Rabat, Morocco
Emails: nabil.akdim@intel.com, cnm@es.aau.dk, benjillali@ieee.org, edc@es.aau.dk

Abstract—We propose an iterative training procedure that approximates multi-stream MIMO eigenmode transmission between two transceivers equipped with hybrid digital analog antenna arrays. The procedure is based on a series of alternate (ping pong) transmissions between the two devices in order to exploit the reciprocity of the wireless channel. During the ping pong iterations, the update of the devices' digital precoders/combiners is performed based on a QR decomposition of the received signal matrix. Concurrently, their analog precoders/combiners are progressively updated by a novel "multi-beam split and drop with backtracking" mechanism that tracks the channel's main spatial components. As shown throughout the paper, the proposed algorithm converges with only few iterations, has minimal computational complexity, and performs very closely to optimal singular value decomposition based precoding with sufficiently large signal-to-noise ratio.

I. INTRODUCTION

Upcoming wireless communication networks are expected to provide service to an unprecendently large number of wireless devices with peak data rates in the order of tens of Gbps. The congestion and fragmentation of the traditional spectral bands below 6GHz has pushed wireless service providers to explore vacant spectrum at the millimeter-wave (mmWave) frequency bands (30–300 GHz) in order to fulfill that goal [1]. Nevertheless, the poor reflectivity and high absorption and free space propagation losses make communicating wirelessly over such high frequencies a challenging task [2]. Fortunately, this frequency range will allow for the use of compact and small antenna arrays with high number of elements, as the physical size of the array is proportional to the carrier wavelength. The large beamforming gains that such large-scale arrays enable will be used to compensate for the above limitations.

However, the high cost, power consumption and complexity of the mixed signal hardware at mm-wave make having large antenna arrays with digitally controlled elements infeasible [3]. This has motivated the wireless communication research community to look at the hybrid digital-analog antenna array architectures [4]. In such architectures, the large antenna array is steered using analog phase shifters and only a few digitally modulated radio-frequency (RF) chains. An illustration of such an architecture is shown in Fig. 1.

In addition to their cost and implementation advantages, hybrid array structures entail their own challenges: the low SNR resulting from high propagation losses, the large dimensionality of the MIMO channel matrix and the presence of analog processing complicate the acquisition of the channel state information (CSI) and the computation of the MIMO precoders and combiners [1], [3]. Luckily, channel measurement campaigns [2] have shown that mm-wave channels are sparse in the angular domain, which enables the proposal of CSI acquisition and precoding/combining algorithms that exploit such property. An example of these are compressed sensing based approaches such as [3], [5], [6], which are generally computationally complex and require a large amount of channel measurements. An alternative are exhaustive and hierarchical beam-search techniques, which may entail significant latency and probability of miss detection [7].

In this work, we focus on a beam training strategy based on alternating transmissions between two transceivers, which has been coined ping pong beam training (PPBT). The main idea behind PPBT is to exploit the reciprocity of the MIMO channel. With appropriate processing at each device, the alternate transmissions implicitly implement an algebraic power iteration that leads to approximating the top left and right singular vectors of the MIMO channel matrix. This idea was first applied in the digital arrays context for single stream wireless communications in [8], [9], and was extended to multi stream setups in [10], to large antenna array and frequency selective systems in [11] and to noisy MIMO channels in [12]. More recently, similar approaches have been proposed in the context of mmWave communications with hybrid digital-analog antenna arrays, which we review next. In [13], the basic ping pong beam training method for single-stream MIMO transmission was adapted to the hybrid array architecture with the inclusion of a "beam split-and-drop" procedure for the setting of analog precoders. The subspace estimation and decomposition method in [14] proposes a ping pong based algorithm that iteratively estimates the channel's right and left eigenvectors using a Krylov subspace estimation method. This algorithm is based on exhaustive measurements with a large set of different analog precoders, which are then
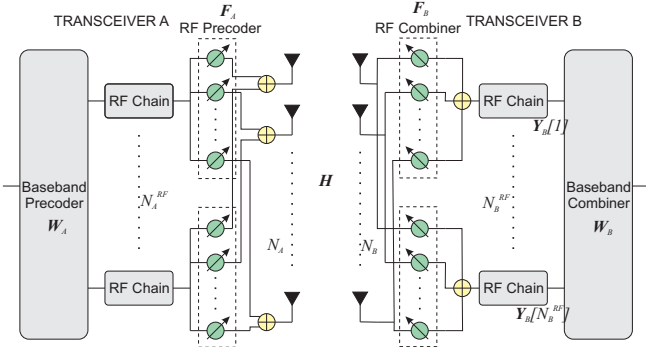
Fig. 1: Structure of the transceivers

linearly combined in order to cancel the effect of the analog precoders. It therefore requires significant amount of transmissions, which imply large signalling overhead and latency. Lastly, the power iteration based training method introduced in [15] is a technique that extends the solution proposed in [10] to the multi stream case, where the digital precoders are set based on an algebraic power iteration technique, while the analog precoders update is done based on a compressed sensing technique called simultaneous orthogonal matching pursuit [16].

Compared to the above approaches, we propose in this article a strategy that sets the digital and analog precoders of the devices in a way to approximate the top N_S left and right singular vectors of the channel matrix, with N_S being the desired number of spatial streams. Our new technique, which we dub *"hybrid ping pong multi beam training"* *(Hybrid PPMBT)* extends the work done in [13] to the multi stream case. It adapts the PPBT strategy to hybrid arrays by progressively choosing the analog precoders at each device from a predefined hierarchical codebook. After one round-trip transmission, a novel *"multi beam split and drop strategy with backtracking"* is applied to focus the analog precoders towards the spatial directions that are most likely containing the channel's top N_S multipath components. The digital precoders are updated via an orthogonal decomposition operation on the received signal as described in [10]. In comparison to the approaches in [14] and [15], Hybrid PPMBT is much simpler from a computational complexity aspect and has a low training overhead as it requires significantly fewer transmissions. Simulation results show that our proposed scheme performs very well in retrieving the wanted N_S channel's top eigenmodes for sufficiently large signal-to-noise ratio, both in terms of accuracy and convergence speed.

II. SYSTEM MODEL

We consider a system in which two hybrid analog digital transceivers A and B, equipped with uniform linear arrays (ULA) composed of N_A and N_B antenna elements. Such elements are separated with a distance $d = \lambda/2$, where λ is the wavelength of interest. The two devices control digitally their arrays with N_A^{RF} and N_B^{RF} RF chains respectively and exchange data over a reciprocal wireless MIMO channel using N_S parallel data streams. The channel from device A to

device B is considered to be static and narrowband and is modeled according to the finite scatterer channel model with L propagation paths [13], [17], as

$$\boldsymbol{H} = \sqrt{\frac{N_A N_B}{L}} \sum_{l=1}^{L} \alpha_l \boldsymbol{a}_B(\Omega_{B,l}) \boldsymbol{a}_A^{\mathrm{H}}(\Omega_{A,l}), \qquad (1)$$

here, $\boldsymbol{H} \in \mathbb{C}^{N_B \times N_A}$, L is the number of multipath components (MPC), α_l is the complex fading channel gain for MPC l, $\Omega_{A,l} = \frac{2\pi}{\lambda} d \cos \phi_{A,l}$ and $\Omega_{B,l} = \frac{2\pi}{\lambda} d \cos \phi_{B,l}$ are the directional cosines corresponding to the lth MPC at arrays A and B respectively, where $\phi_{A,l}$, $\phi_{B,l}$ are the angles of incidence of that same path, and $\boldsymbol{a}_A$ and $\boldsymbol{a}_B$ are the array response vectors at device A and B respectively. The α_l are modeled as independent, standard complex gaussian variables, the $\phi_{A,l}$ and $\phi_{B,l}$ as uniformly distributed in the range $[0, 2\pi)$ radians and the array responses as $\boldsymbol{a}_A(\Omega_{A,l}) = [1, e^{-j\Omega_{A,l}}, \ldots, e^{-j(N_A-1)\Omega_{A,l}}]^{\mathrm{T}}/\sqrt{N_A}$ and $\boldsymbol{a}_B(\Omega_{B,l}) = [1, e^{-j\Omega_{B,l}}, \ldots, e^{-j(N_B-1)\Omega_{B,l}}]^{\mathrm{T}}/\sqrt{N_B}$.

In order to establish the wireless link with device B, device A (we assume, without loss of generality, that device A is performing the first transmission) transmits $\boldsymbol{T}$, an $N_S \times N_S$ orthogonal training sequence i.e $\boldsymbol{T}\boldsymbol{T}^{\mathrm{H}} = \boldsymbol{I}_{N_S}$. Upon reception, device B cancels the training sequence effect by multiplying its received digital signal by $\boldsymbol{T}^H$. The resulting signal can be expressed as:

$$\boldsymbol{Y}_B = \boldsymbol{F}_B^{\mathrm{H}} \boldsymbol{H} \boldsymbol{F}_A \boldsymbol{W}_A + \boldsymbol{F}_B^{\mathrm{H}} \boldsymbol{N}_B, \qquad (2)$$

where $\boldsymbol{F}_A \in \mathbb{C}^{N_A \times N_A^{RF}}$ and $\boldsymbol{F}_B \in \mathbb{C}^{N_B \times N_B^{RF}}$ contain the states of the analog precoder and combiner of transceivers A and B, $\boldsymbol{W}_A \in \mathbb{C}^{N_A^{RF} \times N_S}$ denotes the digital precoder of transceiver A and $\boldsymbol{N}_B \in \mathbb{C}^{N_B \times N_S}$ is a complex, circularly-symmetric additive white gaussian noise matrix, obtained after training sequence removal and with i.i.d elements, each with variance σ^2. Transmissions from device B to device A are modeled analogously as

$$\boldsymbol{Y}_A = \boldsymbol{F}_A^{\mathrm{H}} \boldsymbol{H}^{\mathrm{H}} \boldsymbol{F}_B \boldsymbol{W}_B + \boldsymbol{F}_A^{\mathrm{H}} \boldsymbol{N}_A, \qquad (3)$$

where $\boldsymbol{W}_B \in \mathbb{C}^{N_B^{RF} \times N_S}$ and $\boldsymbol{N}_A \in \mathbb{C}^{N_A \times N_S}$ are defined similar to the above.

III. HYBRID PING PONG MULTI BEAM TRAINING : HYBRID PPMBT

Given the signal model in (2) and (3), the beamforming task consists of selecting the set of analog and digital precoders and combiners that maximize the spectral efficiency over a given channel matrix $\boldsymbol{H}$. For transmission from device A to B, and assuming unit transmit power equally allocated across the N_S streams, the spectral efficiency reads

$$R = \log_2 \det \left(\boldsymbol{I}_{N_S} + \frac{\boldsymbol{R}_{\boldsymbol{N}_B}^{-1}}{N_S} \boldsymbol{H}_e \boldsymbol{H}_e^{\mathrm{H}} \right), \qquad (4)$$

where $\boldsymbol{R}_{\boldsymbol{N}_B} = \sigma^2 \boldsymbol{W}_B^{\mathrm{H}} \boldsymbol{F}_B^{\mathrm{H}} \boldsymbol{F}_B \boldsymbol{W}_B$ is the noise covariance matrix after receive combining at device B, $\boldsymbol{H}_e = \boldsymbol{W}_B^{\mathrm{H}} \boldsymbol{F}_B^{\mathrm{H}} \boldsymbol{H} \boldsymbol{F}_A \boldsymbol{W}_A$ is the equivalent channel after precoding and combining at both devices. An analogous expression applies for transmission from device B to device A.

The optimal precoders maximizing (4) are known to be the N_S top right and left singular vectors of $\boldsymbol{H}$. However, the hybrid structure of the antenna array makes the computation

of such precoders challenging. On the one hand, as digital measurements of the channel are only obtained after analog precoding and combining, estimating the full channel matrix $\boldsymbol{H}$ in order to obtain its singular value decomposition requires a large number of measurements and hence large overhead and latency [14]. On the other hand, even if the channel matrix $\boldsymbol{H}$ can be estimated, the precoders have to be built as the product of the analog precoding matrix $\boldsymbol{F}_A$ and the digital precoding matrix $\boldsymbol{W}_A$. While the elements of $\boldsymbol{W}_A$ can take any complex value due to its digital implementation, the operation modeled by $\boldsymbol{F}_A$ is implemented via phase shifters and combiners, which restricts the values it can take. In this work, we restrict the entries of $\boldsymbol{F}_A$ to satisfy $|(\boldsymbol{F}_A)_{l,i}|$[1] $\in \{\frac{1}{M_A^{(i)}}; 0\}$, where $M_A^{(i)}$ being the number of activated array elements in the ith column of $\boldsymbol{F}_A$, and the option $(\boldsymbol{F}_A)_{l,i} = 0$ accounts for the option of leaving some elements of the array unused. In addition, a transmit power constraint is enforced such that $\|\boldsymbol{F}_A\boldsymbol{W}_A\|_F = 1$.[2] With these constraints, finding the combination of digital and analog precoders to best approximate the channel's singular vectors becomes a computationally intensive optimization problem [5].

To overcome such difficulties, we propose an iterative multi beam training scheme based on alternate transmissions between the two devices, this procedure estimates progressively and simultaneously the top N_S right and left singular vectors of $\boldsymbol{H}$ and sets the digital and analog precoders so that they approach those singular vectors. It consists of two parts: **1)** a *"backtracking beam split and drop"* approach to select the analog precoders $\boldsymbol{F}_A$ and $\boldsymbol{F}_B$ from a predefined multi level codebook, **2)** a method to select the digital precoders $\boldsymbol{W}_A$ and $\boldsymbol{W}_B$ inspired by the $\boldsymbol{QR}$ decomposition algorithm described in [10].

We will proceed by reviewing the beam training procedure for digital antenna arrays proposed in [10], then briefly present the multi level codebook that is used for the analog precoder update, and finally explain our multi beam training solution.

A. Ping-Pong Multi Beam Training with Digital Antenna Arrays: Digital PPMBT

We review the digital PPBT algorithm over a narrowband reciprocal channel $\boldsymbol{H}$ as described in [10]. We consider two devices A and B equipped with digitally controlled antenna arrays with N_A and N_B elements respectively. At the initial (0th) iteration, the process starts with a random initialization of the precoder at device A, $\boldsymbol{W}_A^{[0]}$. A uses then this initial precoder to transmit a training to B. Upon reception and training sequence removal, device A gets an estimate of $\boldsymbol{HW}_A^{[0]}$, makes a $\boldsymbol{QR}$-decomposition on it, and uses the $\boldsymbol{Q}$ part of that decomposition as its precoder $\boldsymbol{W}_B^{[0]}$. It then uses that precoder to transmit a training sequence back to device A, who will repeat the same operations. This process is reiterated until convergence, at which, device A gets an estimate of the

[1]$(\boldsymbol{F}_A)_{l,i}$ is the entry of the matrix $\boldsymbol{F}_A$ belonging to its lth row and ith column.
[2]Obviously, the same constraints apply to the analog precoder of device B.

top N_S right singular vectors of $\boldsymbol{H}$ and device B gets an estimate of the top N_S right singular vectors of $\boldsymbol{H}^{\mathrm{H}}$. Further details on this procedure can be found in [10].

Algorithm 1 Ping Pong Multi Beam Training with Hybrid Arrays

$$\boldsymbol{F}_A^{[0]} \leftarrow \left[\boldsymbol{\varphi}_{A,0}^{(1)}, \boldsymbol{\varphi}_{A,1}^{(1)}, \ldots, \boldsymbol{\varphi}_{A,M_A^{(1)}-1}^{(1)}\right],$$
$$\boldsymbol{F}_B^{[0]} \leftarrow \left[\boldsymbol{\varphi}_{B,0}^{(1)}, \boldsymbol{\varphi}_{B,1}^{(1)}, \ldots, \boldsymbol{\varphi}_{B,M_B^{(1)}-1}^{(1)}\right],$$

1: **Initialize:** Initialize $\boldsymbol{W}_A^{[0]}$ to an orthogonal matrix of its size.
    for $s = 1 : N_S$ **do**
$$\boldsymbol{W}_A^{[0]}(:,s) \leftarrow \frac{\boldsymbol{W}_A^{[0]}(:,s)}{\sqrt{N_S}\left\|\boldsymbol{F}_A^{[0]}\boldsymbol{W}_A^{[0]}(:,s)\right\|_2}$$
    end for
    $\{\boldsymbol{p}_A, \boldsymbol{k}_A, \boldsymbol{i}_A\} \leftarrow \{[], [], []\}, \{\boldsymbol{p}_B, \boldsymbol{k}_B, \boldsymbol{i}_B\} \leftarrow \{[], [], []\}$.
2: A transmits, B receives: $\boldsymbol{Y}_B^{[0]} = (\boldsymbol{F}_B^{[0]})^{\mathrm{H}}\boldsymbol{HF}_A^{[0]}\boldsymbol{W}_A^{[0]} + (\boldsymbol{F}_B^{[0]})^{\mathrm{H}}\boldsymbol{N}_B^{[0]}$
3: $[\boldsymbol{Q}, \boldsymbol{R}] \leftarrow qr(\boldsymbol{Y}_B^{[0]})$
4: **for** $s = 1 : N_S$ **do**
5:     $\boldsymbol{W}_B^{[0]}(:,s) \leftarrow \boldsymbol{Q}(:,s)$
6:     $\boldsymbol{W}_B^{[0]}(:,s) \leftarrow \frac{\boldsymbol{W}_B^{[0]}(:,s)}{\sqrt{N_S}\left\|\boldsymbol{F}_B^{[0]}\boldsymbol{W}_B^{[0]}(:,s)\right\|_2}$
7: **end for**
8: $t \leftarrow 1$
9: **loop**
10:     B transmits,
11:     A receives $\boldsymbol{Y}_A^{[t]} = (\boldsymbol{F}_A^{[t-1]})^{\mathrm{H}}\boldsymbol{H}^{\mathrm{H}}\boldsymbol{F}_B^{[t-1]}\boldsymbol{W}_B^{[t-1]} + (\boldsymbol{F}_A^{[t-1]})^{\mathrm{H}}\boldsymbol{N}_A^{[t]}$
12:     $[\boldsymbol{Q}, \boldsymbol{R}] \leftarrow qr(\boldsymbol{Y}_A^{[t]})$
13:     **for** $s = 1 : N_S$ **do**
14:         $\boldsymbol{W}_A^{[t]}(:,s) \leftarrow \boldsymbol{Q}(:,s)$
15:         $\boldsymbol{W}_A^{[t]}(:,s) \leftarrow \frac{\boldsymbol{W}_A^{[t]}(:,s)}{\sqrt{N_S}\left\|\boldsymbol{F}_A^{[t-1]}\boldsymbol{W}_A^{[t]}(:,s)\right\|_2}$
16:     **end for**
17:     $[\boldsymbol{F}_B^{[t]}, \{\boldsymbol{p}_B, \boldsymbol{k}_B, \boldsymbol{i}_B\}]$ $\leftarrow$ UPD.AN.PR$(\boldsymbol{F}_B^{[t-1]}, \boldsymbol{W}_B^{[t-1]}, \mathcal{C}_B, \{\boldsymbol{p}_B, \boldsymbol{k}_B, \boldsymbol{i}_B\})$
18:     A transmits,
19:     B receives: $\boldsymbol{Y}_B^{[t]} = (\boldsymbol{F}_B^{[t]})^{\mathrm{H}}\boldsymbol{HF}_A^{[t-1]}\boldsymbol{W}_A^{[t]} + (\boldsymbol{F}_B^{[t]})^{\mathrm{H}}\boldsymbol{N}_B^{[t]}$
20:     $[\boldsymbol{Q}, \boldsymbol{R}] \leftarrow qr(\boldsymbol{Y}_B^{[t]})$
21:     **for** $s = 1 : N_S$ **do**
22:         $\boldsymbol{W}_B^{[t]}(:,s) \leftarrow \boldsymbol{Q}(:,s)$
23:         $\boldsymbol{W}_B^{[t]}(:,s) \leftarrow \frac{\boldsymbol{W}_B^{[t]}(:,s)}{\sqrt{N_S}\left\|\boldsymbol{F}_B^{[t]}\boldsymbol{W}_B^{[t]}(:,s)\right\|_2}$
24:     **end for**
25:     $[\boldsymbol{F}_A^{[t]}, \{\boldsymbol{p}_A, \boldsymbol{k}_A, \boldsymbol{i}_A\}]$ $\leftarrow$ UPD.AN.PR$(\boldsymbol{F}_A^{[t-1]}, \boldsymbol{W}_A^{[t]}, \mathcal{C}_A, \{\boldsymbol{p}_A, \boldsymbol{k}_A, \boldsymbol{i}_A\})$
26:     $t \leftarrow t + 1$
27: **end loop**

B. Analog Precoder Multi Level Codebook

We illustrate here the codebook definition for transceiver A (an analogous codebook is used for the transceiver B). We consider a codebook $\mathcal{C}_A$ which is composed of $L_A = \log_2(N_A/N_A^{RF}) + 1$[3] levels. For the kth level, we define a subcodebook $\mathcal{C}_A^{(k)} = \{\boldsymbol{\varphi}_{A,i}^{(k)}, i=0, 1, \ldots, M_A^{(k)}-1\}$ consisting of $M_A^{(k)} = N_A^{RF}2^{k-1}$ column vectors, $k=1, 2, \ldots, L_A$. Each of the elements of the subcodebook is defined as

[3]For the considered codebook design we constrain N_A and N_A^{RF} to be both integer powers of two.

$$\varphi_{A,i}^{(k)} = \left[1, e^{-j\psi_{A,i}^{(k)}}, \dots, e^{-j(M_A^{(k)}-1)\psi_{A,i}^{(k)}}, \mathbf{0}_{N_A-M_A^{(k)}}^{\mathrm{T}}\right]^{\mathrm{T}} / \sqrt{M_A^{(k)}},$$

where $\psi_{A,i}^{(k)} = \pi - \pi(2i+1)/M_A^{(k)}$ is the directional cosine of the ith vector at the kth level ($\varphi_{A,i}^{(k)}$ steers the array in the direction $\theta_{A,i}^{(k)} = \arccos \psi_{A,i}^{(k)}/\pi$, with a lobe whose width decreases with the codebook level k), and $\mathbf{0}_N$ is the N-dimensional column zero vector. Further details about the codebook used here can be found in [13].

C. Ping Pong Multi Beam Training with Hybrid Antenna Arrays : Hybrid PPMBT

The proposed algorithm for beam training with hybrid arrays is described in pseudocode. Algorithm 1 presents the overall training scheme, while Algorithm 2 describes the subroutine used to update the analog precoding matrices.

1) Initialization: First, the digital and analog precoders are initialized. $\boldsymbol{F}_A$ and $\boldsymbol{F}_B$ are initialized to $\mathcal{C}_A^{(1)}$ and $\mathcal{C}_B^{(1)}$ respectively, while $\boldsymbol{W}_A$ is initialized to a random unitary matrix. The columns of $\boldsymbol{W}_A$ are then normalized to fulfill the transmit power constraint of the effective precoder $\boldsymbol{F}_A\boldsymbol{W}_A$. Finally, a set of empty arrays, $\{\boldsymbol{p}_B, \boldsymbol{k}_B, \boldsymbol{i}_B\}$, are created. Those arrays will store the needed information to perform the analog precoder updates, as explained below.

2) Ping Pong Iterations: After the initialization phase, a sequence of alternate pilot transmissions starts between the two devices. The baseband precoders are updated after each reception step by means of a $\boldsymbol{QR}$-decomposition, followed by a normalization step. These two operations are detailed in lines 3-7, 12-16 and 20-24 in Algorithm. 1. Immediately after updating their baseband precoders upon reception of a transmission, the devices transmit back with the updated digital precoders and the same analog precoder as used for reception. Only after the transmission has been made will the transmitting device update its analog precoders (using Algorithm 2), such that next reception is done with the updated setting. This allows for the $\boldsymbol{QR}$ based iteration to converge, as each reception-transmission cycle is performed over a static setting of the analog precoders.

3) Update of Analog Precoders: The devices invoke the routine outlined in Algorithm 2 to update their analog precoder state. This routine bases its update on the current state of the device's RF precoder $\boldsymbol{F}$, its codebook $\mathcal{C}$ and on the update history of its baseband precoder $\boldsymbol{W}$. Using all previous updates of $\boldsymbol{W}$ allows for **backtracking**–i.e, correcting for wrong RF precoder updates. The routine works as follows:

a) Three sequences of values are generated: k_n stores the level of the codebook of the nth column of $\boldsymbol{F}$, p_n stores the squared norm of the nth row of $\boldsymbol{W}$, i.e the aggregate energy received on it, and i_n stores the index of the nth column of $\boldsymbol{F}$, out of the level of the codebook to which that column belongs.

b) The sequences generated above will be used to update three vectors: k_n will be appended to $\boldsymbol{k}$, with $\boldsymbol{k}$ being an array storing the codebook levels of the columns of $\boldsymbol{F}$ used over consecutive ping-pong iterations. p_n will be appended to $\boldsymbol{p}$, with $\boldsymbol{p}$ being an array storing the received energy over the different spatial directions set by the analog beamformer $\boldsymbol{F}$. i_n will be appended to $\boldsymbol{i}$ in a similar manner to the above.

c) Once $\boldsymbol{p}$ is updated, it will be sorted in a descending manner and the resulting sorted indices will be stored in $\boldsymbol{p}_I$. This newly formed array will be used to find the entries of $\boldsymbol{p}$ that are most likely to direct the analog precoders where the MPCs of $\boldsymbol{H}$ are.

d) Two new vectors are built: $\boldsymbol{b}_I$ contains the K first indexes of $\boldsymbol{p}_I$ i.e it identifies the beams that are most aligned with the channel's MPCs (K is the length of $\boldsymbol{b}_I$, which can be derived from lines 9-13). $\boldsymbol{b}_L$ is a vector that is made of 1's and 2's. The ith entry of $\boldsymbol{b}_L$ is set to 2 when the precoder corresponding to the ith entry of $\boldsymbol{b}_I$ is replaced with the two precoders belonging to one step higher level of the codebook and that have their beams covering together its same spatial area, otherwise it is set to 1. Deciding to append 1 or 2 to $\boldsymbol{b}_L$ depends on whether we already consumed all columns of $\boldsymbol{F}$ and on whether the element of $\boldsymbol{p}_I$ in question belong to the last level of the codebook or not (see lines 17-21). Line 8 of the algorithm erases the measurement stored over a beam that is selected to be included in the analog precoding matrix, either directly or after splitting it into two beams of the immediately higher level. As new measurements will be obtained over that beam in the next iteration, the old measurement is deleted to avoid unnecessarily coming back to the previous configuration corresponding to that

---

Algorithm 2 Analog Precoder Update

1: **function** UPD.AN.PR($\boldsymbol{F}$, $\boldsymbol{W}$, $\mathcal{C}$, $\{\boldsymbol{p},\boldsymbol{k},\boldsymbol{i}\}$)
2:     **Generate** : $k_n, i_n, p_n, n=1,\dots,N^{RF}$, where k_n will store the codebook level to which the $\boldsymbol{F}'s$ n^{th} column belongs, i_n will store its index out of that level and p_n will store the norm of the nth row of $\boldsymbol{W}$, i.e the aggregate energy received on it.
3:     $\boldsymbol{p} \leftarrow [\boldsymbol{p}, p_1, \dots, p_{N^{RF}}]$, $\boldsymbol{k} \leftarrow [\boldsymbol{k}, k_1, \dots, k_{N^{RF}}]$, $\boldsymbol{i} \leftarrow [\boldsymbol{i}, i_1, \dots, i_{N^{RF}}]$
4:     Sort $\boldsymbol{p}$ in a descending manner and store the result in $\boldsymbol{p}_S$, then store the arrangement of the elements of $\boldsymbol{p}$ into $\boldsymbol{p}_S$ in $\boldsymbol{p}_I$.
5:     $\boldsymbol{b}_I \leftarrow []$, $\boldsymbol{b}_L \leftarrow []$
6:     **while** $n \leq N^{RF}$ **do**
7:         $\boldsymbol{b}_I \leftarrow [\boldsymbol{b}_I, p_{I,n}]$, $p_{I,n}$ is the nth element of $\boldsymbol{p}_I$,
8:         $p_{p_{I,n}} \leftarrow 0$, $p_{p_{I,n}}$ is the $p_{I,n}$th element of $\boldsymbol{p}$,
9:         **if** $k_{p_{I,n}} = \log_2(\frac{N}{N^{RF}})+1$ or $n=N^{RF}$-1 **then**
10:           $n \leftarrow n+1$, $\boldsymbol{b}_L \leftarrow [\boldsymbol{b}_L, 1]$
11:         **else**
12:           $n \leftarrow n+2$, $\boldsymbol{b}_L \leftarrow [\boldsymbol{b}_L, 2]$
13:         **end if**
14:     **end while**
15:     **for** $t = 1 : \text{Length}(\boldsymbol{b}_I)$ **do**
16:         $m \leftarrow b_{L,t}$
17:         **if** $m = 2$ **then**
18:           $\boldsymbol{F} \leftarrow [\boldsymbol{F}, \varphi_{2i_m}^{(k_m+1)}, \varphi_{2i_m+1}^{(k_m+1)}]$
19:         **else**
20:           $\boldsymbol{F} \leftarrow [\boldsymbol{F}, \varphi_{i_m}^{(k_m)}]$
21:         **end if**
22:     **end for**
23:     **return** $\{\boldsymbol{F}; \{\boldsymbol{p}, \boldsymbol{k}, \boldsymbol{i}\}\}$
24: **end function**

old measurement.

e) Finally, the RF precoder columns are updated (lines 15-22).

We dub the above procedure for updating the analog precoders "*beam split and drop with backtracking*", owing to the way it operates. At each iteration, a decision is made as to whether a given beam is split –i.e replaced by two more directive beams– or dropped –i.e. removed from the precoding matrix. The *backtracking* feature refers to the fact that, via the vector $\boldsymbol{p}$, the measurements obtained in prior ping-pong iterations are kept in memory, allowing for returning to lower level beams in the codebook in the cases where noise leads to erroneous decisions in the the split-and-drop procedure.

IV. NUMERICAL RESULTS

In order to assess the effectiveness of the proposed algorithm, we perform Monte Carlo simulations for multiple configurations of the hybrid arrays at devices A and B. The channel matrix $\boldsymbol{H}$ follows the model in (1). The average SNR for the sth stream link between the nth element of the array at device B and the mth element of the array at A is defined as $\rho=\mathbb{E}\{|H_{nm}|^2\}/\mathbb{E}\{|N_{ns}|^2\}=1/\sigma^2$, where N_{ns} is the nth entry of the sth column of the noise matrix $\boldsymbol{N}$. We assume here for simplicity that the SNR ρ is the same for all streams. H_{nm} is the channel coefficient between device B's nth array element and device A's mth array element, and $\mathbb{E}\{\}$ is the expectation operator.

We measure the performance with the average spectral efficiency per bits/s/Hz, expressed with $\log_2\left(\left|\boldsymbol{I}_{N_S}+\frac{\boldsymbol{R}_N^{-1}}{N_S}\boldsymbol{H}_e\boldsymbol{H}_e^{\mathrm{H}}\right|\right)$, where $\boldsymbol{H}_e=(\boldsymbol{F}_B^{[n-1]}\boldsymbol{W}_B^{[n-1]})^{\mathrm{H}}\boldsymbol{H}\boldsymbol{F}_A^{[n-1]}\boldsymbol{W}_A^{[n]}$ and $\boldsymbol{R}_N=\sigma^2(\boldsymbol{F}_B^{[n-1]}\boldsymbol{W}_B^{[n-1]})^{\mathrm{H}}\boldsymbol{F}_B^{[n-1]}\boldsymbol{W}_B^{[n-1]}$ for integer iteration n, and $\boldsymbol{H}_e=(\boldsymbol{F}_B^{[n]}\boldsymbol{W}_B^{[n]})^{\mathrm{H}}\boldsymbol{H}\boldsymbol{F}_A^{[n-1]}\boldsymbol{W}_A^{[n]}$ and $\boldsymbol{R}_N=\sigma^2(\boldsymbol{F}_B^{[n]}\boldsymbol{W}_B^{[n]})^{\mathrm{H}}\boldsymbol{F}_B^{[n]}\boldsymbol{W}_B^{[n]}$ for half iteration $n+0.5$.

We benchmark the performance of the hybrid PPMBT against the performance of the digital ping pong multi stream beam training method (digital PPMBT) described in [10], for which the spectral efficiency is calculated in a similar manner to that of the hybrid PPMBT. We compare it also with the optimal unconstrained SVD based precoder, which maximize the spectral efficiency and which is obtained by using the top N_S left and right singular vectors of $\boldsymbol{H}$. Note that the SVD based precoder derivation requires full channel knowledge at both devices, an information that is hard to get when hybrid architectures are used as explained earlier, and which our proposed scheme does not need at the start, but rather learns while setting the precoders.

We start our evaluation in the high SNR regime (ρ=30dB), in which the training process will not be impaired too much by noise. This allows assessing how the arrays size, the number RF chains and the number of spatial streams really affect the algorithm's performance.

Fig. 2 depicts the algorithm's performance over a channel with 8 multipath components, when the two devices are
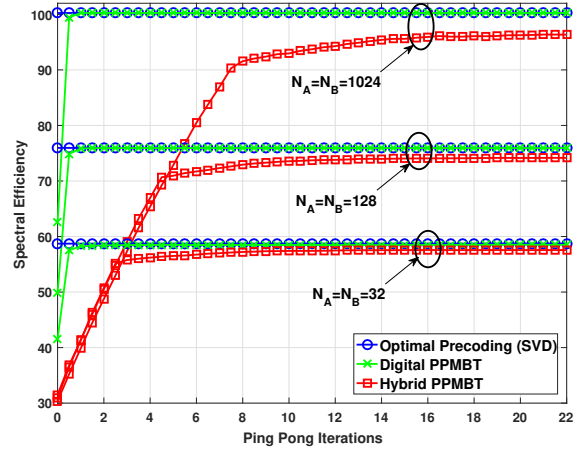

Fig. 2: Spectral Efficiency (bits/s/Hz) attained by the algorithm over PP Iterations. Devices A and B are equipped with a hybrid array. $N_A^{RF}=N_B^{RF}=8, N_S=4, L=8, \rho=$30dB.

equipped with identical arrays made of $N_A=N_B=$32, 128 or 1024 elements and a fixed number of RF chains $N_A^{RF}=N_B^{RF}=$8 and try to establish an $N_S=4$ streams MIMO communication. We see that the algorithm reaches, in very few iterations, for small, medium and large sized arrays, to about 1 to 2 bits/s/Hz of the digital PPMBT and SVD based precoding schemes performances. We also see that the convergence speed (in terms of PP iterations) scales inversely to the codebook depth for each of the topologies: the convergence is slower when large arrays are used because, in such cases, the codebook has more levels and its few last levels contain a high number of beamformers with very narrow beams. The selection of such directive beams is more prone to error than those in codebooks with lower resolution. Although the backtracking mechanism can correct for the errors made, this comes at the expense of a larger number of iterations needed for convergence. Note that the number of PP iterations needed for convergence for all topologies is still much below what is needed for exhaustive search: this latter requires as an example, for $N_A=N_B=$1024 with $N_A^{RF}=N_B^{RF}=$8, $N_A/N_A^{RF}=N_B/N_B^{RF}=$128 PP iterations to find the best beams, compared with only 16 for our algorithm.

Fig. 3 shows the algorithm's performance over the same channel as the one used in Fig. 2, but with the number of MIMO streams, N_S, taking different values (4, 6 and 8) and the two devices being equipped with identical arrays made of $N_A=N_B=$128 elements and use 8 RF chains each. The purpose of these simulations is to investigate how does the ratio of the number of MIMO streams to the number of RF chains N_S/N_{RF} affect the algorithm's performance. We can clearly see that the algorithm behaves in three different ways depending on the aforementioned ratio: **1)** When $N_S \leq N_{RF}/2$, the convergence is very quick and no backtracking is performed. **2)** When $N_{RF}/2 < N_S < N_{RF}$, the algorithm's convergence is slowed down and one observes some irregularity of the convergence behavior over iterations which is due to the
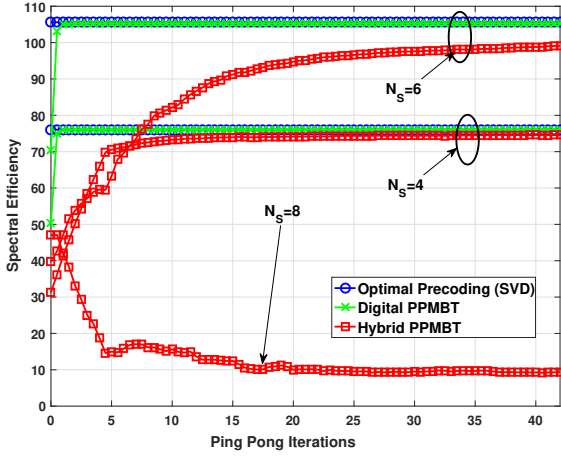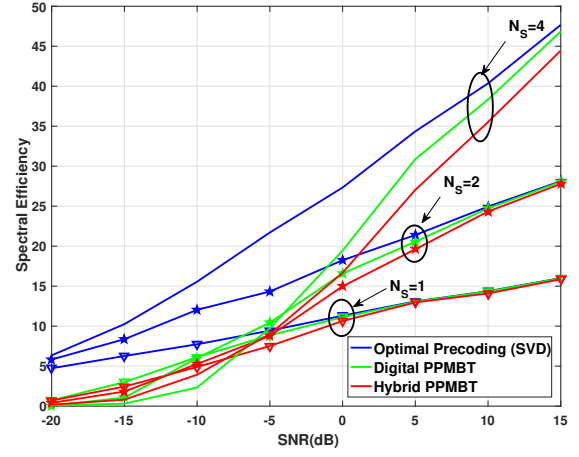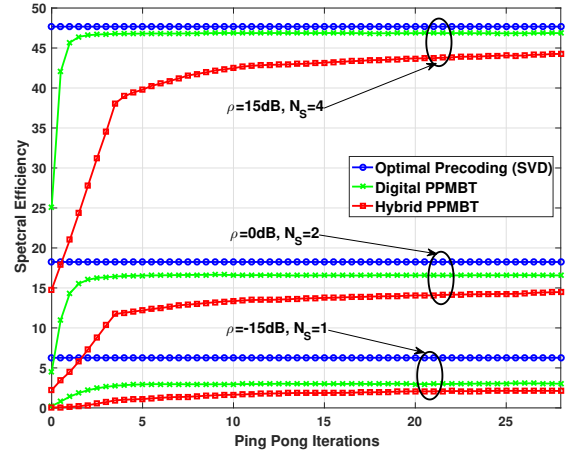
Fig. 3: Spectral Efficiency (bits/s/Hz) attained by the algorithm over PP Iterations for different N_S values. Devices A and B are equipped with a hybrid array. $N_A=N_B=128$, $N_A^{RF}=N_B^{RF}=8$, $L=8$, $\rho=30$dB.

backtracking mechanism. **3)** When $N_{RF} = N_S$, the algorithm fails to provide acceptable performance.

Next, in Fig. 4, we fix the size of antenna arrays and number of RF chains used at both devices to $N_A=N_B=64$ and $N_A^{RF}=N_B^{RF}=8$, and evaluate the algorithm's performance over a channel with $L = 7$ multipath components at different SNR values. In Fig. 4a, we show the algorithm's performance against SNR after training convergence for different N_S values. The results show that the number of streams that the training algorithm can handle efficiently grows with SNR, as is to be expected. At low SNR regimes (-15 to 0 dB) the algorithm works better when it attempts to estimate only the dominant singular vector of the channel; if more singular vectors are estimated, the large estimation error degrades the overall spectral efficiency of the system. As the SNR grows, an increasing number of singular vectors can be accurately estimated by the algorithm and, hence, increasing the number of streams provides significant spectral efficiency gains. For all cases, we observe that the performance of the Hybrid PPMBT is very close to that of the fully-digital counterpart, and approaches the SVD precoding performance as the SNR grows. In Fig. 4b the convergence behavior of the training algorithm with different N_S settings is evaluated at their respective SNR values of interest. We observe that the method's spectral efficiency tends to saturate at around 10 ping pong iterations for moderate and high SNR. Convergence for lower SNR values is, however, slower. We attribute this effect to the fact that the large noise power induces numerous incorrect beam selection errors in the updates of the analog precoder; although the backtracking feature of the algorithm can help correct some of them, the price to pay is a longer training time. In any case, we remark that the algorithm reaches about 70% of the spectral efficiency obtained at convergence within the first 6 iterations, regardless of the SNR value and number of spatial streams.

(a)

(b)

Fig. 4: Spectral Efficiency (bits/s/Hz) attained by the algorithm over PP Iterations for different N_S values. Devices A and B are equipped with a hybrid array. $N_A=N_B=64$, $N_A^{RF}=N_B^{RF}=8$, $L=7$. (a):Spectral Efficiency over SNR, (b): Spectral Efficiency over PP Iterations

To conclude, we evaluate our proposed training procedure in a system in which only one of the devices is equipped with a large, hybrid array ($N_A=256$, $N_A^{RF}=16$), while the other has a digitally-controlled array of moderate size ($N_B=4$). Such topologies can be seen as massive MIMO systems operating at microwave frequencies. In addition, to reflect the richer scattering experienced in such frequency bands [18], we adopt the following channel model:

$$\boldsymbol{H}=\frac{\sqrt{N_A N_B}}{L}\boldsymbol{A}_B\boldsymbol{\Lambda}\boldsymbol{A}_A^{\mathsf{H}} \tag{5}$$

where $\boldsymbol{A}_A$ contains in its columns the steering vectors $\boldsymbol{a}_A(\Omega_{A,p}), p=1,2,\ldots,P$, $\boldsymbol{A}_B$ is defined analogously, L is again the number of multipath components, and $\boldsymbol{\Lambda}$ is a $L \times L$ matrix with i.i.d. standard complex Gaussian entries. This setting will allow to test the validity of our approach in channels with richer scattering and its robustness against the sparse assumption of the channel.
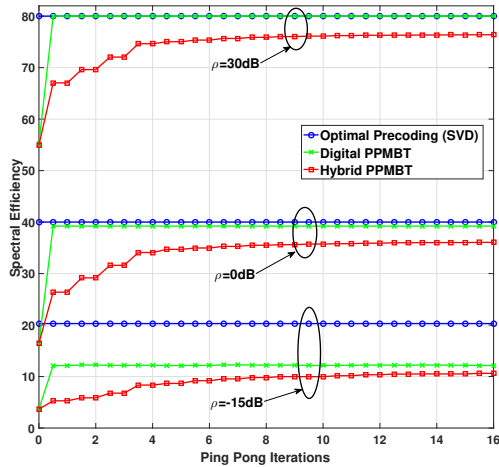
Fig. 5: Spectral Efficiency (bits/s/Hz) attained by the algorithm over PP Iterations. Device A is equipped with a hybrid array and device B has a full digital architecture. N_A=128, N_B=4, N_A^{RF}=16, N_S=4, L=40.

Fig. 5 shows the algorithm's performance over a rich scattering channel (L=40) when N_A=128, N_A^{RF}=16, $N_B=N_S$=4. It can be seen that the proposed scheme performs remarkably well and very close to the full digital and optimal SVD based precoder solutions at low, mid and high SNRs. These results show that, although the algorithm was originally designed to exploit the sparse nature of mmWave channels, it is robust to channels with richer scattering.

V. CONCLUSION

We proposed a method to derive precoders and combiners for multi-stream MIMO transmission between two devices equipped with hybrid digital-analog antenna arrays. The method relies on a low-complexity "multi-beam split and drop with backtracking" procedure to update the analog precoders, while digital precoders are computed with the QR-decomposition based method in [10]. For sufficiently large SNR, the resulting precoders approximate well the unconstrained SVD-based precoders, as our numerical assessment shows. We envision that the proposed algorithm can be especially useful in mmWave communication systems.

Compared to the state-of-art methods, our approach offers the advantage of computational simplicity while achieving high-spectral efficiency with moderate training overhead. The numerical results show that the method achieves convergence within $N^{RF}(\log_2(N/N^{RF})+1)$ ping pong iterations in the low SNR regime and $\log_2(N/N^{RF})+1$ iterations in the mid and high SNR regime, assuming both transceivers are equipped with arrays made of N elements and N^{RF} RF chains. Although the method was developed with sparse channels in mind, the performance assessment shows that it is robust against this assumption and also performs well in rich scattering channels.

Also, in order to further reduce the training overhead, the proposed scheme can be interleaved with transmission of payload with increasing data-rate. This, the extension to multi-user environments and to time varying channels will be the subject of our future work.

REFERENCES

[1] T. S. Rappaport, S. Sun, R. Mayzus, H. Zhao, Y. Azar, K. Wang, G. N. Wong, J. K. Schulz, M. Samimi, and F. Gutierrez, "Millimeter wave mobile communications for 5G cellular: It will work!" *IEEE Access*, vol. 1, pp. 335–349, 2013.

[2] S. Hur, S. Baek, B. Kim, Y. Chang, A. F. Molisch, T. S. Rappaport, K. Haneda, and J. Park, "Proposal on millimeter-wave channel modeling for 5G cellular systems," *IEEE Journal of Selected Topics in Signal Processing*, vol. 10, no. 3, pp. 454–469, Apr. 2016.

[3] R. W. Heath, N. González-Prelcic, S. Rangan, W. Roh, and A. M. Sayeed, "An overview of signal processing techniques for millimeter wave MIMO systems," *IEEE Journal of Selected Topics in Signal Processing*, vol. 10, no. 3, pp. 436–453, Apr. 2016.

[4] X. Zhang, A. F. Molisch, and S.-Y. Kung, "Variable-phase-shift-based RF-baseband codesign for MIMO antenna selection," *IEEE Transactions on Signal Processing*, vol. 53, no. 11, pp. 4091–4103, Nov. 2005.

[5] O. E. Ayach, S. Rajagopal, S. Abu-Surra, Z. Pi, and R. W. Heath, "Spatially sparse precoding in millimeter wave MIMO systems," *IEEE Transactions on Wireless Communications*, vol. 13, no. 3, pp. 1499–1513, Mar. 2014.

[6] A. Alkhateeb, O. E. Ayach, G. Leus, and R. W. Heath, "Channel estimation and hybrid precoding for millimeter wave cellular systems," *IEEE Journal of Selected Topics in Signal Processing*, vol. 8, no. 5, pp. 831–846, Oct. 2014.

[7] M. Giordani, M. Mezzavilla, and M. Zorzi, "Initial access in 5G mmwave cellular networks," *IEEE Communications Magazine*, vol. 54, no. 11, pp. 40–47, November 2016.

[8] J. B. Andersen, "Intelligent antennas in a scattering environment – an overview," in *IEEE Global Communications Conference (GLOBECOM)*, Sydney, Australia, Nov. 1998, pp. 3199–3203 (vol. 6).

[9] ——, "Array gain and capacity for known random channels with multiple element arrays at both ends," *IEEE Journal on Selected Areas in Communications*, vol. 18, no. 11, pp. 2172–2178, Nov. 2000.

[10] T. Dahl, N. Christophersen, and D. Gesbert, "Blind MIMO eigenmode transmission based on the algebraic power method," *IEEE Transactions on Signal Processing*, vol. 52, no. 9, pp. 2424–2431, Sep. 2004.

[11] E. de Carvalho and J. B. Andersen, "Ping-pong beam training for reciprocal channels with delay spread," in *49th Asilomar Conference on Signals, Systems and Computers*, Pacific Grove, CA, USA, Nov. 2015, pp. 1752–1756.

[12] D. Ogbe, D. J. Love, and V. Raghavan, "Noisy beam alignment techniques for reciprocal MIMO channels," *IEEE Transactions on Signal Processing*, vol. 65, no. 19, pp. 5092–5107, Oct. 2017.

[13] C. N. Manchón, E. de Carvalho, and J. B. Andersen, "Ping-pong beam training with hybrid digital-analog antenna arrays," in *IEEE International Conference on Communications (ICC)*, Paris, France, May 2017, pp. 1–7.

[14] H. Ghauch, T. Kim, M. Bengtsson, and M. Skoglund, "Subspace estimation and decomposition for large millimeter-wave MIMO systems," *IEEE Journal of Selected Topics in Signal Processing*, vol. 10, no. 3, pp. 528–542, Apr. 2016.

[15] X. Cheng, N. Lou, and S. Li, "Spatially sparse beamforming training for millimeter wave MIMO systems," *IEEE Transactions on Wireless Communications*, vol. 16, no. 5, pp. 3385–3400, May 2017.

[16] M. F. Duarte and Y. C. Eldar, "Structured compressed sensing: From theory to applications," *IEEE Transactions on Signal Processing*, vol. 59, no. 9, pp. 4053–4085, Sept 2011.

[17] A. G. Burr, "Capacity bounds and estimates for the finite scatterers MIMO wireless channel," *IEEE Journal on Selected Areas in Communications*, vol. 21, no. 5, pp. 812–818, Jun. 2003.

[18] J. Andersen, "Propagation aspects of MIMO channel modeling," in *Space-Time Wireless Systems*, H. Bolcskei, C. Papadias, D. Gesbert, and A.-J. van der Veen, Eds. Cambridge University Press, 2006, ch. 1.